Integrated vs Decoupled Fault Detection Filter & Flight Control Law Designs for a Re-Entry Vehicle

Helena Castro, Samir Bennani and Andrés Marcos

***Abstract*— An integrated design of a robust fault detection filter and control system for a re-entry vehicle is presented. The integrated architecture is based on the four-block Youla parametrization which allows to better and directly trade-off filter and control design objectives in the face of disturbances and uncertainties. $\mathcal{H}_\infty$-optimization techniques are used to design the integrated controller/filter system for a re-entry vehicle with actuator faults in the transonic flight regime where the aerodynamics are highly uncertain. Finally the resulting integrated controller/filter properties are compared with a decoupled fault detection filter and flight control designs. The integrated design obtained successfully identifies the desired faults for the nominal and uncertain cases. Moreover, the integrated design minimizes the faults effects on the system response better than the decoupled design. Lastly, it is clearly shown that the actuator activity is directly related with the faults introduced.**

I. Introduction

One of the main challenges in the fault detection and fault tolerant control fields is to develop detection algorithms that are able to distinguish between faults, disturbances, system noise and model uncertainties. When talking about disturbances and model uncertainties one plausible approach that immediately springs to mind is the H_∞ framework. The standard H_∞-based robust control design approach results in a single LTI controller where one of the important design decisions is the trade-off between performance and robustness. Indeed, it is well known in the robust control community that the robustness of a closed-loop system design is usually achieved at the expense of its performance. Nevertheless, for the case of model uncertainty and typical exogenous disturbances (i.e. noise, wind, friction, etc) the H_∞ control design technique is well established and numerous example of its application exists.

However, when an additional control requirement is tolerance to faults (whereby it is expected that the closed-loop performance will not be affected by faults or at least will remain stable) the standard H_∞ robust control design represents a passive approach since the faults are not directly considered in the design set-up. Within this passive approach faults that can be characterized as strong disturbances, to which the control system was designed to be robust, can be tolerated by the closed loop. However, in this way the performance for the no-fault case will be highly penalized since robust control takes into account worst-case scenarios. A better approach relies on the detection of the faults in order to introduce fault-feedback compensation or control reconfiguration based on the fault information to keep at least stability if performance is not possible. This is known as the active approach.

An approach developed throughout the last ten years [1], [3], [4], [7] which uses H_∞ robust control design for fault tolerance purposes in an active manner is the so-called integrated control and filter design. This is based on the four-parameter controller proposed in [1], a full generalization of the standard two degrees-of-freedom (DoF) Youla controller which incorporates an additional two DoF for diagnostic purposes. It can be shown [2] that the optimal integrated design is equal to the optimal non-integrated design of the controller and detection filter if there is no model uncertainty. When there is uncertainty (indeed always) the design is coupled and then the integrated approach [3] presents a more advantageous framework for the trade-off between performance and robustness, furthermore there are also gains in terms of implementation and reliability.

An alternative implementation of the integrated control which also allows for a very nice decoupling between nominal high-performance and robust (to fault or uncertainty) controllers was presented in [4]. More recently the integrated controller has been developed in a linear fractional transformation [6] formulation which allows for easier analysis and design and also enables the development of advanced scheduling techniques [8]. Despite this ample theoretical development around the integrated controller, only a few available references of its application to complex systems can be found, see [7] and references therein.

In this paper the design of an integrated robust FDI filter and flight control system for a re-entry vehicle in landing phase during which actuator faults in different channels occur is investigated. In section II, the four-parameter Youla parametrization is presented together with the LFT representation used for design the integrated filter/controller. Section III presents the re-entry model and defines the disturbances and uncertainties weights that act upon the model. On Section IV a brief description and some results of a non-integrated filter design [10] is given, while the integrated filter/controller design is presented in Section V. A

H. Castro and S. Bennani are with ESA-ESTEC, Keplerlaan 1, 2200 AG Noordwijk, The Netherlands. {helena.castro, samir.bennani}@esa.int

A. Marcos started this work while at the University of Leicester, Leicester, LE2 2LG, UK, he is now with the Advanced Projects Division at Deimos-Space S.L., Ronda Poniente 19, Ed. Fiteni VI, 28760 Madrid, Spain. andres.marcos@deimos-space.com

comparison between the non-integrated and integrated design using time simulation responses is presented in Section VI.

II. Problem Formulation

A state space description of $G(s)$ can be formulated as:

$$G(s) = \left(\begin{array}{c|cc} A & B_1 & B_2 \\ \hline C_1 & D_{11} & D_{12} \\ C_2 & D_{21} & D_{22} \end{array} \right) \tag{1}$$

or given as transfer functions:

$$\left(\begin{array}{c} e \\ y \end{array} \right) = \left(\begin{array}{cc} G_{ed}(s) & G_{eu}(s) \\ G_{yd}(s) & G_{yu}(s) \end{array} \right) \left(\begin{array}{c} d \\ u \end{array} \right) \tag{2}$$

The model $G(s)$ contains both the nominal model and weight matrices for the disturbance and performance specifications. In a standard design, a controller $K(s)$ is designed such that the closed loop is internally stable and a suitable norm of the closed loop transfer function is minimized.

However, now we are interested in integrating the filter design into the controller design. The approach for the synthesis of a controller with fault detection capabilities enables the designer to explicitly address the interactions between both systems, which for the uncertain case are known to be coupled, [2].

Several approaches exist in the literature all related to the Youla parametrization. The four-parameter structure was first used by Nett *et al.*, [1]. The theory used here is taken from [6], [7] and [8]. The four-parameter controller is a generalization of the Youla parametrization which extends the controller to four degrees of freedom. These are: 1) reference signal tracking, 2) closed-loop stabilization, 3) residual generation and 4) disturbance rejection. The structure of the four-block parametrization is shown in figure 1. The general result is formalized in the following Theorem.

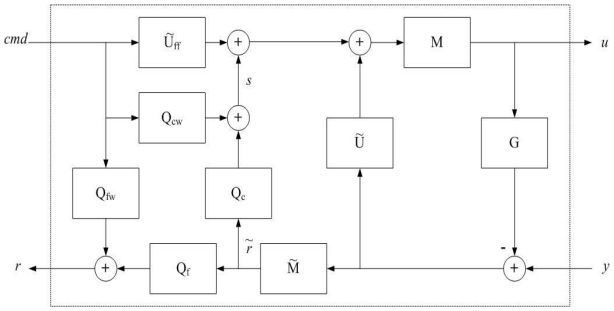

Fig. 1. Four-parameter controller structure

Theorem 1: **General Four-Parameter Controller** *Consider a nominal plant $G \in \Re_p$. Assume a corresponding nominal stabilizing controller, $K_o \in \Re_p$, and feedforward controller, $K_{ff} \in \Re_p$, are given. Let any right/left coprime factorization for the nominal plant, $G_u = M^{-1}N = \tilde{N}\tilde{M}^{-1}$, and controllers, $K_o = V^{-1}U = \tilde{U}\tilde{V}^{-1}$, $K_{ff} = V^{-1}U_{ff} = \tilde{U}_{ff}\tilde{V}^{-1}$, be also known. The class of all proper integrated stabilizing and residual generator controllers, $K_F(Q) \in \Re_p$, is parameterized by:*

$$\left[\begin{array}{c} u \\ r \end{array} \right] = \left[\begin{array}{c} (\tilde{V} + Q_c\tilde{N}_u)^{-1}(\tilde{U} + Q_c\tilde{M}) \\ Q_f \left(\tilde{M} - \tilde{N}_u(\tilde{V} + Q_c\tilde{N}_u)^{-1}(\tilde{U} + Q_c\tilde{M}) \right) \\ (\tilde{V} + Q_c\tilde{N}_u)^{-1}(\tilde{U}_{ff} + Q_{cw}) \\ Q_{fw} - Q_f\tilde{N}_u(\tilde{V} + Q_c\tilde{N}_u)^{-1}(\tilde{U}_{ff} + Q_{cw}) \end{array} \right] \left[\begin{array}{c} y \\ cmd \end{array} \right] \tag{3}$$

Under the following conditions $\left(\tilde{V} + Q_c\tilde{N}_u\right)(\infty)$ exist and

$$\left[\begin{array}{c} s \\ r \end{array} \right] = Q \left[\begin{array}{c} \tilde{r} \\ cmd \end{array} \right] = \left[\begin{array}{cc} Q_c & Q_{cw} \\ Q_f & Q_{fw} \end{array} \right] \left[\begin{array}{c} \tilde{r} \\ cmd \end{array} \right] \in \Re H_\infty \tag{4}$$

where u is the feedback control input, r the residual vector, y the plant measurements and cmd the exogenous input.

In [6], Marcos and Balas show that the above general integrated controller parametrization can be formulated as a lower fractional transformation (LFT), $K_F(Q) = F_l(\tilde{J}, Q)$, where the free matrix Q is given by equation (4) and the coefficient matrix $\tilde{J}$ is given as follow:

$$\left[\begin{array}{c} u \\ r \\ \tilde{r} \\ cmd \end{array} \right] = \left[\begin{array}{cccc} \tilde{V}^{-1}\tilde{U} & \tilde{V}^{-1}\tilde{U}_{ff} & \tilde{V}^{-1} & 0 \\ 0 & 0 & 0 & I \\ V^{-1} & -\tilde{N}_u\tilde{V}^{-1} & 0 & \\ 0 & I & 0 & 0 \end{array} \right] \left[\begin{array}{c} y \\ cmd \\ s \\ r \end{array} \right] \tag{5}$$

This LFT formulation allows for a more transparent look at the interactions between control and diagnosis objectives.

III. Re-entry Vehicle Model

The re-entry vehicle (RV) model is taken from [9]. It represents a simplified lateral-directional rigid-body model of the Space Shuttle, in the final stages of landing as it transitions from supersonic to subsonic speeds.

The equations of motion are linearized at Mach 0.9 and the state-space model is given by a four-state vector: sideslip angle β, roll rate p, yaw rate r, and bank angle ϕ; three inputs: commanded elevon deflection θ_{ele}, rudder deflection command θ_{rud} and lateral wind/gust disturbance d_{gust}; and four output measurements: roll and yaw rate states, lateral acceleration n_y and the bank angle. An input/output block diagram of the aircraft is shown in figure 2.

The actuators for each of the two controlled inputs, θ_{ele} and θ_{rud}, are modeled with a second order transfer function, as well as a second order delay approximation to model the effects of digital implementation, see Chapter 7 in [9] for more details. Similarly, the output signals are measured with inertial measurement units (IMU) and navigation derived air data sensors (NAVDAD) whose noise characteristics become more severe with increasing frequency. The p and r signals are measured with comparable gyroscopes while the

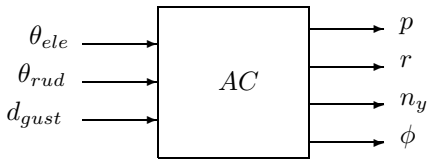

Fig. 2. Aircraft block diagram

measurement of ϕ is obtained from the navigation package at a reduced sample rate. In order to simulate environmental effects, the exogenous input signal, d_{gust}, is used to model lateral wind gusts typically encountered at this flight condition:

$$d_{gust} \in \{W_{gust}\delta_{gust} : ||\delta_{gust}||_2 \leq 1\} \tag{6}$$

$$W_{gust} = 30\frac{1+s/2}{1+s} \tag{7}$$

The re-entry vehicle model just described will be used for controller/filter design and nominal LTI simulation (it is highlighted that 'nominal' includes sensor noise, actuator time delay and gust disturbances). To test the robustness properties –to model mismatch or uncertainty– of the designs we will introduce uncertainty in the nominal LTI model.

The major source of uncertainty in the aircraft model is in the aerodynamic coefficients. At this flight condition (i.e. transonic regime) theoretical, computational, and wind-tunnel techniques are inaccurate. Thus, uncertainty in the aerodynamic coefficients is modeled as a nominal value plus a perturbation as shown in equation (8). The perturbations δ_{ij} are assumed to be fixed, unknown, real parameters, each satisfying $|\delta_{ij}| < 1$.

$$\begin{pmatrix} c_{y_\beta} & c_{y_a} & c_{y_r} \\ c_{\eta_\beta} & c_{\eta_a} & c_{\eta_r} \\ c_{l_\beta} & c_{l_a} & c_{l_r} \end{pmatrix} = \begin{pmatrix} \bar{c}_{y_\beta} & \bar{c}_{y_a} & \bar{c}_{y_r} \\ \bar{c}_{\eta_\beta} & \bar{c}_{\eta_a} & \bar{c}_{\eta_r} \\ \bar{c}_{l_\beta} & \bar{c}_{l_a} & \bar{c}_{l_r} \end{pmatrix} + \\ + \begin{pmatrix} r_{y_\beta}\delta_{y_\beta} & r_{y_a}\delta_{y_a} & r_{y_r}\delta_{y_r} \\ r_{\eta_\beta}\delta_{\eta_\beta} & r_{\eta_a}\delta_{\eta_a} & r_{\eta_r}\delta_{\eta_r} \\ r_{l_\beta}\delta_{l_\beta} & r_{l_a}\delta_{l_a} & r_{l_r}\delta_{l_r} \end{pmatrix} \tag{8}$$

The aerodynamic coefficient perturbation matrix can be written as a LFT where the nine perturbation parameters δ_{ij} are placed on a structured uncertainty matrix, i.e. everywhere zero except along the main diagonal which contains the $\delta'_{ij}s$. Again, see reference [9] for more details.

IV. Non-Integrated Controller and FDI filter Design

In this section we briefly cover the baseline non-integrated designs of the vehicle's attitude controller and FDI filter. They are taken from [9] and [10] respectively.

Typically, a vehicle of these characteristics follows a re-entry reference trajectory that the control system is in charge of tracking – mainly using attitude commands, i.e. bank angle and angle of attack while keeping sideslip to zero. A critical phase in the re-entry profile involves a series of sweeping "S" turns in order to slow down the vehicle as it enters the Earth atmosphere. These, also called bank-reversal, manoeuvres may involve changes in the bank angle of up to $\pm$ 80 degrees or more and due to the high speed of the vehicle they place stringent constraints on the actuator effort. Additionally, due to flying and comfort considerations, it is also required to perform coordinated turns and to minimize lateral acceleration.

Therefore, the controller objectives are to achieve accurate tracking of bank-angle commands, good turn coordination, very little acceleration and small actuator signals. Three controllers were obtained in [9] using $\mathcal{H}_\infty$-optimization and D-K iteration techniques. We will use the controller obtained through $\mathcal{H}_\infty$-optimization (in that reference is called k_x) and refer to it as the non-integrated controller or k_{Nint}. We highlight that this non-integrated controller is designed to be robust to model uncertainty and environmental effects (e.g. noise and gust) but no active or direct fault accommodation was considered in its design.

Next, in order to select the fault scenario we look at the re-entry profile and select the flight phase corresponding to the lower part of the reference trajectory, e.g. Mach numbers below 2.5 and dynamic pressure higher than 1400 Pa, where the reaction control system (RCS) is not active any more and the control of the vehicle is performed through the aerodynamic surfaces. Therefore, the diagnosis objectives of the non-integrated FDI filter F_{Nint} are to detect and isolate faults in the elevon and rudder actuators. The diagnostic channels were designed to be decoupled from each other, be robust to uncertainty, and be able to reject or attenuate disturbances. The faults are assumed to enter the system in an additive manner and a model-matching formulation [5] is used, see [10] for more details. It is highlighted that this represents a very challenging problem as the control aerodynamic surfaces are formed by (two) flaps and (two) rudders which couple in order to provide motion along the three body axes.

Figure 3 shows the time responses of the closed loop formed by the non-integrated controller k_{Nint} and the nominal and uncertain LTI models from Section III under a fault environment. A zero bank angle command is used to better observe fault effects on the system time response. The faults, together with the diagnosis responses of the non-integrated filter F_{Nint}, are given in Figure 4.

Notice that the response of the controller is affected by the introduction of faults, see especially the less-than-perfect bank angle tracking and the small peaks throughout the n_y response. Also, notice that there seems to be not much difference between the nominal and uncertain plant output responses. Nevertheless, the diagnostic residuals are quite different for both cases: quite good detection for the nominal plant but noticeable degradation for the uncertain

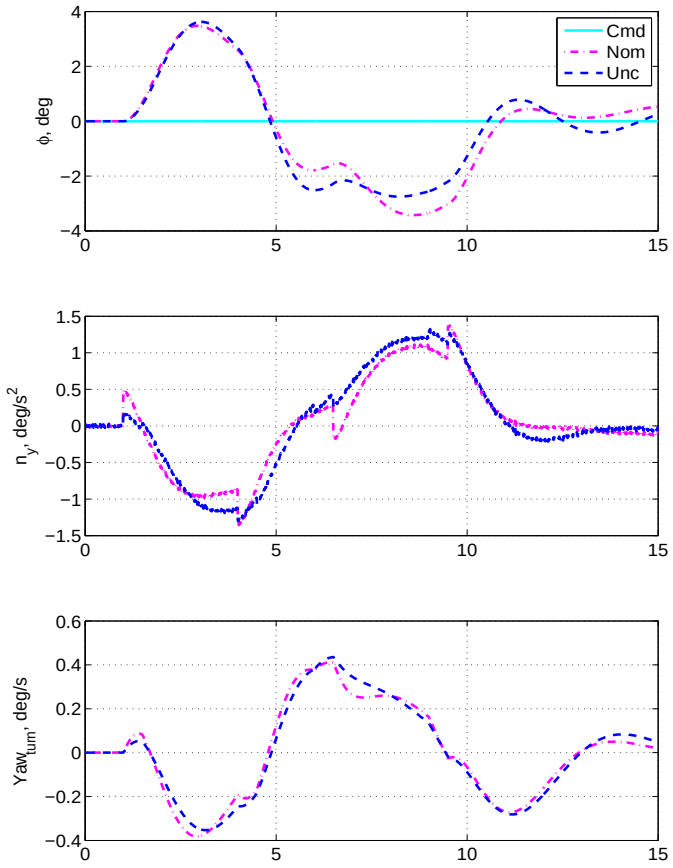

Fig. 3. System Responses for K_{Nint} with nominal and uncertain plants.

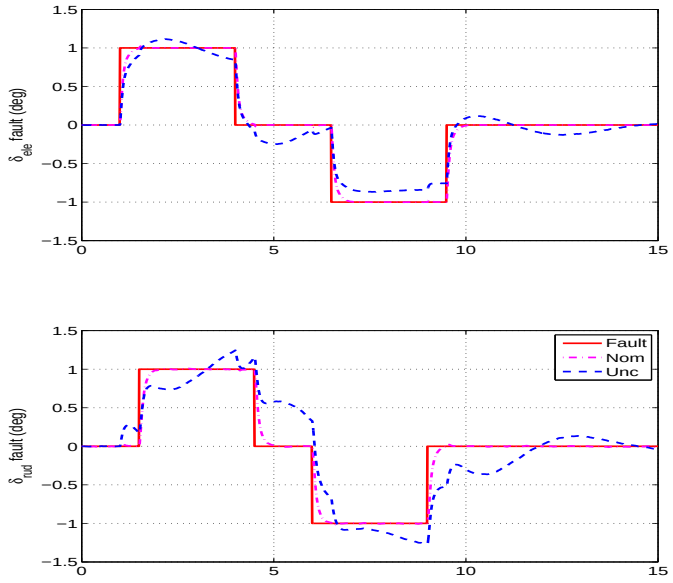

Fig. 4. Residuals of F_{Nint} with nominal and uncertain plants.

case (esteeming from residual –and indirectly, command–coupling), for further details refer to [10].

V. Integrated Filter-Controller Design

In this section, the integrated design of the control and FDI filter is provided. The integrated design K_{Int} has certain advantages compared with the non-integrated design as mentioned before, not the least important that the control design can accommodate faults. The design approach used follows that of references [3], [7] and the objectives and initial baseline weight designs are taken from the non-integrated designs of the previous section.

Therefore, the controller is designed to follow accurately an ideal bank angle response. This ideal bank angle response is given by equation (9), with $\omega = 1.2rad/sec$ and $\zeta = 0.7$.

$$\phi_{ideal} = \frac{1}{s^2 + 2\zeta\omega s + \omega^2}\phi_{cmd} \tag{9}$$

For accuracy the bank-angle commands are further modeled as

$$\phi_{cmd} = W_{\phi_{cmd}}\delta_{\phi_{cmd}} \tag{10}$$

$$W_{\phi_{cmd}} = 0.5\frac{1 + s/2}{1 + s/0.5} \tag{11}$$

This transfer weighting function implies that the bank-angle commands are dominated by low frequency signals, with a maximum magnitude of approximately 0.5 radians. Turn coordination error is defined as follows:

$$r_p = r - 0.037\phi \tag{12}$$

Furthermore, since it is desired very little lateral acceleration, then the lateral acceleration variable, n_y, is defined also as an error. The performance error signals are then weighted by frequency dependent weights to give a performance error signal:

$$e_p = W_p \begin{bmatrix} n_y \\ r - 0.037\phi \\ \phi - \phi_{ideal} \end{bmatrix} \tag{13}$$

where

$$W_p = \begin{bmatrix} 0.005 & 0 & 0 \\ 0 & 500\frac{1+s}{1+s/0.01} & 0 \\ 0 & 0 & 200\frac{1+s}{1+s/0.01} \end{bmatrix} \tag{14}$$

The angular position for the rudder and elevon surfaces should remain reasonably small in face of the exogenous signals. These signals are weighted to give the following actuator error signal:

$$e_{act} = \begin{bmatrix} 1 & 0 \\ 0 & 0.1 \end{bmatrix} \begin{bmatrix} \theta_{ele} \\ \theta_{rud} \end{bmatrix} \tag{15}$$

With respect to the specific weights for the diagnosis objectives, the following are chosen. The ideal fault models are:

$$f_{ideal} = \begin{bmatrix} \frac{s/40+20}{s+20*0.75} & 0 \\ 0 & \frac{s/50+20}{s+20*0.55} \end{bmatrix} \begin{bmatrix} f_{ele} \\ f_{rud} \end{bmatrix} \tag{16}$$

The filter error is then given by equation (17):

$$e_f = \begin{bmatrix} 1 & 0 \\ 0 & 0.8 \end{bmatrix} \begin{bmatrix} f_{ele} - f_{e_{ele}} \\ f_{rud} - f_{e_{rud}} \end{bmatrix} \tag{17}$$

In the same way as for the non-integrated controller and filter cases, no parametric uncertainty is used in the design of the integrated controller/filter. A multiplicative uncertainty at the actuators input was also used in this design. However, here the weighting functions are selected equal for both channels, and to avoid increasing the number of states, as constants of value 0.1. Furthermore, the noise weights are also changed:

$$W_{p_{ns}} = 0.0003\frac{1+s/0.01}{1+s/0.5} \tag{18}$$

$$W_{roll_{ns}} = 0.0001 \tag{19}$$

$$W_{ny_{ns}} = 0.05\frac{1+s/0.05}{1+s/10} \tag{20}$$

$$W_{\phi_{ns}} = 0.0007\frac{1+s/0.01}{1+s/0.2} \tag{21}$$

The exogenous inputs to the interconnection are the sensors noise vector, the gust disturbance, the command signal and the fault signals. The interconnection exogenous outputs are the error channels for the control and the diagnosis objectives. There are four integrated filter-controller outputs: two signals for feedback control, and two diagnosis signals.

Using the weighting functions defined above, an $\mathcal{H}_\infty$-optimization synthesis was performed resulting in an integrated design with $\gamma = 1.179$.

VI. Results and Discussion

The integrated filter/controller designed in the previous section is compared in this section with the non-integrated controller and filter designs from Section IV.

Again, in order to more easily compare the fault tolerance characteristics of the designs a zero bank angle command is used. In this manner any deviation from zero in the system responses will indicate the fault effects that the feedback controller component could not compensate. The fault scenario used is the same as in Section IV, i.e. square fault inputs for the elevon and rudder.

Finally, in order to test the robustness characteristics of the non-integrated design fifty percent of a worst-case parametric uncertainty from [9] is used. It corresponds to the LFT representation given in Section III with the nine uncertain δ's given by:

$$\begin{aligned} &diag[\delta_{y\beta}, \delta_{\eta\beta}, \delta_{l\beta}, \delta_{ya}, \delta_{\eta a}, \delta_{la}, \delta_{yr}, \delta_{\eta r}, \delta_{lr}] = \\ &diag(-1,-1,-1,1,1,1,-1,-1,-1) * 0.5 \end{aligned} \tag{22}$$

Figures 5 and 6 show respectively the residuals responses and the system responses for the nominal and uncertain integrated controller K_{Int} together with the response of the nominal non-integrated designs K_{Nint}.

It is noted that the FDI characteristics of the integrated design is as good as the nominal response of the non-integrated design, see figure 5. Indeed, the bandwidths of the K_{int} residuals have been increased w.r.t. that of F_{Nint} to enable faster estimation of the faults. It is noted that there is some small coupling between the residuals for the uncertain case but it does not preclude a good identification of the faults.

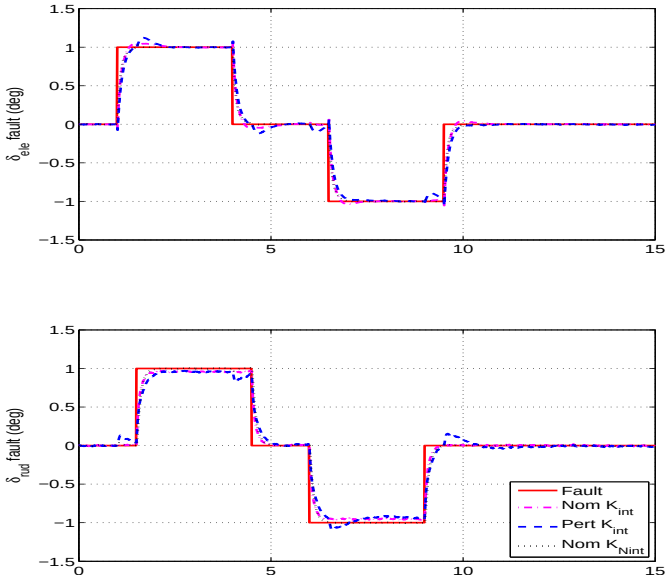

Fig. 5. Fault detection for integrated and non-integrated designs

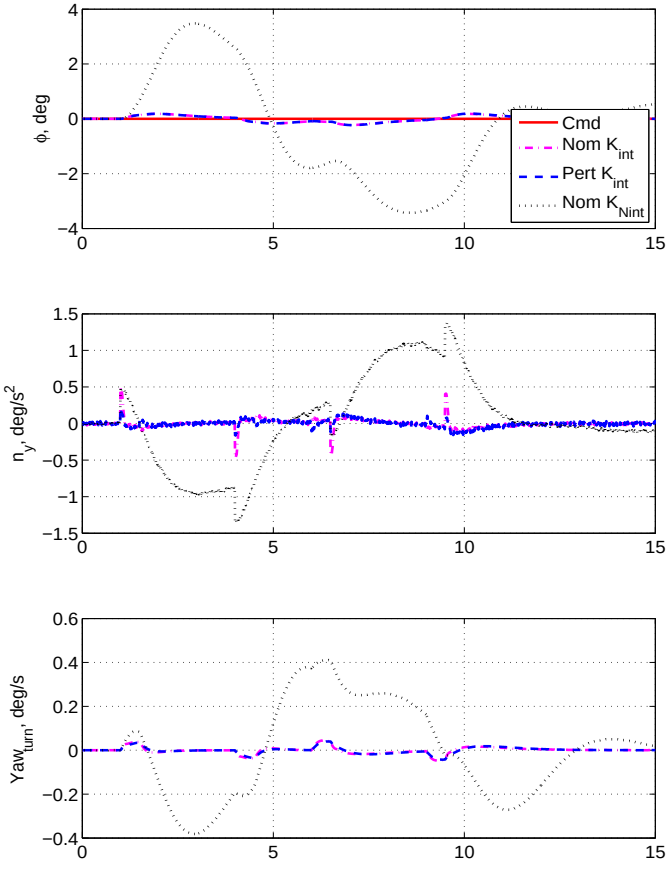

Fig. 6. System performance for integrated and non-integrated designs

Figure 6 shows that since the faults were now directly

considered in the design set-up, the obtained integrated controller is much better in rejecting the effects of the faults. Notice that only small fault effects are visible in the K_{Int} system responses (for both nominal and uncertain cases) while for the nominal K_{Nint} design the previous undesirable fault effects that the controller is not able to reject are observed.

Figure 7 shows the actuator commanded outputs magnitude, θ_{ele} and θ_{rud}. All are similar although the K_{Int} design shows a slightly stronger control authority (longer and stronger use of the actuators) but it is well within limits and of course, it represents the required actuator effort to compensate for the fault effects.

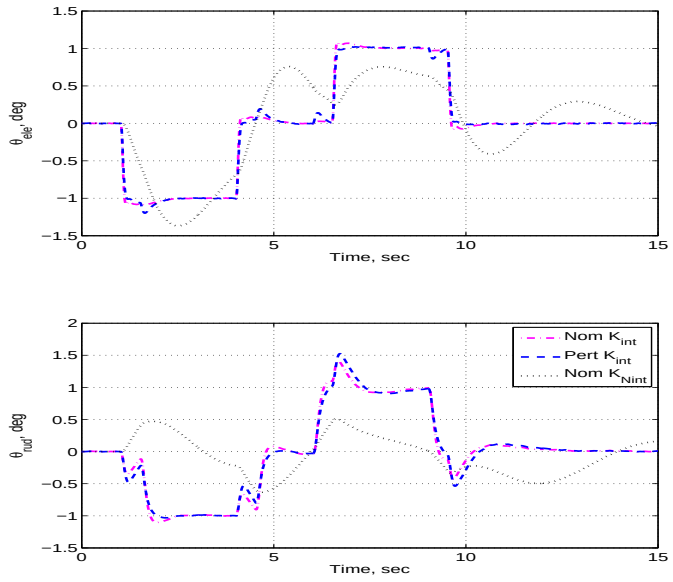

Fig. 7. Actuator signals for integrated and non-integrated designs

Therefore, the integrated design is successful in terms of identifying the faults and rejecting their effects for the nominal and uncertain cases. Nevertheless, although not shown here, both the K_{Nint} and K_{Int} design suffer from command coupling which will need to be corrected through re-design or using fault thresholds. Indeed, due to the large parametric uncertainty considered, the coupling of the aerodynamic surfaces, and the limited number of measured signals available it is not possible to satisfy all the requirements in the design. It is highlighted that this limitation is independent of the design approach and thus negative command decoupling was considered acceptable. Specifically, it is believed that the unavailability of additional measurement signals prevents the fulfilment of all the objectives since the faults considered will show strong effects on the longitudinal motion (i.e. an elevon fault might result in pitching motion while a rudder fault might result in horizontal speed changes) which could have been used to satisfy them.

The reason why the lack of command decoupling is acceptable is that command signals are well-known (and easily measurable) and can be compensated using adaptive thresholds that remove their effects from the fault residuals. Alternatively, weighting functions in the command input could have been used during the designs in order to decrease the filter sensitivity to commands.

VII. Conclusions

In this paper an integrated controller and FDI filter has been designed, and compared to an equivalent non-integrated design, for a re-entry vehicle characterized by a high level of motion coupling and uncertainty, wide operating envelope and limited control surfaces. The vehicle characteristics, fault scenario and the limited number of measurement signals provide a very challenging problem which allows to showcase the usefulness of $\mathcal{H}_\infty$ optimization techniques for the design of fault tolerant integrated control/filter designs. The design thus obtained successfully identifies the desired faults and also rejects the fault effects on the system for the nominal and uncertain cases. Although the integrated filter/controller design shows to be the most successful of both designs, in practice industry does not follow this approach since controllers and filters are usually designed by different groups. However, using nested architectures as in [8], the Youla parametrization principle could still be used in such independent approach.

References

[1] C. N. Nett, C. A. Jacobson and A. T. Miller, "An integrated approach to controls and diagnostics: The 4-parameter controller", in *Proceedings of the American Control Conference*, pp. 824-835, 1988.

[2] H. Niemann and J. Stoustrup, "Integration of control and fault detection: Nominal and robust design", in *IFAC Fault Detection, Supervision and Safety for Technical Processes Symposium*, Kingston Upon Hull, UK, pp. 331-336, 1997.

[3] J. Stoustrup, M. J. Grimble and H. Niemann, "Design of integrated systems for the control and detection of actuator/sensor faults", in *Sensor Review*, Vol 17, No. 2, pp. 138-149, 1997.

[4] K. Zhou and Z. Ren, "A new controller architecture for high performance, robust, and fault-tolerant control", *in IEEE Transactions on Automatic Control*, Vol. 46, No. 10, pp. 1613-1618, October 2001.

[5] A. Marcos, S. Ganguli and G. J. Balas, "An Application of H-infinity Fault Detection and Isolation to a Transport Aircraft", in *Control Engineering Practice*, Vol. 13, No. 1, pp. 105-119, 2005.

[6] A. Marcos and G. J. Balas, "Linear fractional transformation formulation of the integrated controller approach", in *UKACC Control*, Bath, UK, 2004.

[7] A. Marcos and G. J. Balas, "A robust integrated controller/diagnosis aircraft application", in *International Journal of Robust and Nonlinear Control*, **15**:531-551, 2005.

[8] A. Marcos and G. J. Balas, "Nested integrated control and diagnostic filter design", in *Conference on Decision and Control*, 2005.

[9] G. Balas, J. C. Doyle, K. Glover, A. Packard and R. Smith, "*μ-Analysis and Synthesis Toolbox*", Natick, MA: MUSYN, Inc., and The MathWorks, Inc., 1991.

[10] H. V. Castro, S. Bennani, and A. Marcos, "Robust filter design for a re-entry vehicle", in *Proceedings of the 7th International Conference on Dynamic and Control of Systems and Structures in Space*, UK, 16-20 July, 2006.